

THEORY OF VALENCE TRANSITIONS IN  
YTTERBIUM AND EUROPIUM INTERMETALLICS\*

V. ZLATIĆ

Institute of Physics, 10000 Zagreb, P.O. Box 304, Croatia

AND J.K. FREERICKS

Department of Physics, Georgetown University, Washington, DC 20057, USA

*(Received June 21, 2001)*

The exact solution of the multi-component Falicov–Kimball model in infinite-dimensions is presented and used to discuss a new fixed point of valence fluctuating intermetallics with Yb and Eu ions. In these compounds, temperature, external magnetic field, pressure, or chemical pressure induce a transition between a metallic state with the  $f$ -ions in a mixed-valent (non-magnetic) configuration and a semi-metallic state with the  $f$ -ions in an integral-valence (paramagnetic) configuration. The zero-field transition occurs at the temperature  $T_V$ , while the zero-temperature transition sets in at the critical field  $H_c$ . We present the thermodynamic and dynamic properties of the model for an arbitrary concentration of  $d$ - and  $f$ -electrons. For large  $U$ , we find a MI transition, triggered by the temperature or field-induced change in the  $f$ -occupancy.

PACS numbers: 71.30.+h, 75.20.Hr

**1. Introduction**

Intermetallic compounds like YbInCu<sub>4</sub> [1–5] and EuNi<sub>2</sub>(Si<sub>1-x</sub>Ge<sub>x</sub>) [6, 7] exhibit valence-change transitions with dramatic effects on their thermodynamic and transport properties at ambient pressure and low temperatures. One characteristic behavior is seen in the magnetic susceptibility which increases with a Curie-like or Curie–Weiss-like law from high temperatures up to the transition temperature  $T_V$  where it changes to a Pauli-like law with one to two orders of magnitude drop at the transition. Similarly, a magnetic field, for  $T < T_V$ , induces a meta-magnetic transition where the magnetization increases rapidly in a field on the order of a few Tesla.

---

\* Presented at the XII School of Modern Physics on Phase Transitions and Critical Phenomena, Łądek Zdrój, Poland, June 21–24, 2001.

In the high-temperature phase the Yb ions are close to the  $3+ (4f^{13})$  configuration with one paramagnetic ( $J = 7/2$ ,  $L = 3$ ,  $S = 1/2$ )  $f$ -hole, while the Eu ions are close to the  $2+ (4f^7)$  configuration which has one paramagnetic ( $J = 7/2$ ,  $L = 0$ )  $f$ -electron. X-ray edge and Mossbauer spectroscopies indicate a valence change occurs at  $T_V$ ; this change is typically about 0.1 for  $\text{YbInCu}_4$  and 0.6 for  $\text{EuNi}_2(\text{Si}_{1-x}\text{Ge}_x)$ . The volume change of the lattice at the transition roughly agrees with the change in the size of the rare-earth ion assuming that the low-temperature phase of Yb ions contains a mixture of magnetic  $3+$  and non-magnetic  $2+ (4f^{14})$  configurations, and in the Eu compounds a mixture of the magnetic  $2+$  and non-magnetic  $3+ (4f^6)$  states. The surprising feature is that despite the presence of well defined local moments there is no sign of the Kondo effect in the high temperature phase: the electrical resistance is large and with a positive (temperature) slope, the thermoelectric power is small, the magneto-resistance is positive, and the Hall coefficient is large [2–5]. Hence, the high-temperature phase seems to be a semi-metal consisting of conduction electrons that scatter off of  $f$ -electron ions with well defined moments that behave nearly independently.

As the temperature is reduced, the local moments become unstable, and the system undergoes a transition to a low-temperature valence-fluctuating metal that no longer possesses local moments. Magnetic and neutron scattering experiments [8] show that the loss of moment in the low-temperature phase is not due to the onset of any long-range order. The low-temperature phase is metallic with a low resistivity and a small Hall coefficient, but with a large peak in the thermopower. This loss of  $f$ -electron moment occurs not due to a complete transfer of the  $f$ -electron into the conduction band, but rather occurs due to the additional formation of a hybridized valence-fluctuating phase with a quenched magnetic moment. But this valence-fluctuating phase is not an ordinary one, because it is sensitive to external perturbations like a magnetic field which can easily restore the local moments via a meta-magnetic transition or hydrostatic (and chemical) pressure which stabilizes the  $f$ -electron shell with a local moment. Finally, optical conductivity measurements [9] show a complete reconstruction of the many-body excitations as one passes through  $T_V$ , where a mid-infrared peak instantly appears in the low-temperature phase and a Drude peak sharpens and increases its spectral weight.

A complete theoretical description of these systems poses quite a challenge. The creation of a valence-fluctuating state in a conventional periodic Anderson model is robust and insensitive to external perturbations like temperature, magnetic field, or pressure. Transitions from the valence-fluctuating state to any other phase are all believed to be continuous cross-overs that are never first-order-like. On the other hand, the stabilization of intermediate-valence states in the Falicov–Kimball [10] (FK) model is

problematic in the limit as  $T \rightarrow 0$ , since the  $f$ -electrons are usually completely filled or empty in the homogeneous ground state phases. This is true even though the Falicov–Kimball model is known to possess discontinuous valence-change transitions. A proper treatment of these valence fluctuating systems requires combining the periodic Anderson model with the Falicov–Kimball model, by introducing  $d$ – $f$  Coulomb interactions in the former or hybridization in the latter. Solving such a model, and evaluating the phase diagram as a function of all of its parameters is difficult, even with the advanced techniques of dynamical mean field theory. Here we choose an alternate, and hence incomplete approach, which nevertheless appears to capture the majority of the interesting behaviors of these remarkable compounds. We choose to describe these materials by a spin one-half Falicov–Kimball model. We will see below what properties can be described by this model, and more importantly, we point out all of the pitfalls that arise due to the neglect of the hybridization. We give reasonable arguments about how we expect hybridization to modify the behavior below.

The Falicov–Kimball Hamiltonian is

$$H = -\frac{t^*}{2\sqrt{d}} \sum_{\langle i,j \rangle \sigma} d_{i\sigma}^\dagger d_{j\sigma} + E_f \sum_{i\sigma} f_{i\sigma}^\dagger f_{i\sigma} + U \sum_{i\sigma\sigma'} f_{i\sigma}^\dagger f_{i\sigma} c_{i\sigma'}^\dagger c_{i\sigma'}, \quad (1)$$

where  $d_{i\sigma}^\dagger$  ( $d_{i\sigma}$ ) is the electron creation (annihilation) operator for an electron at site  $i$  with spin  $\sigma$ ,  $E_f$  is the energy level of the localized electrons (not to be confused with a Fermi energy),  $f$  labels the corresponding  $f$ -electron creation and annihilation operators, and  $U$  is the interaction strength. The total  $f$ -electron occupation is restricted to be less than or equal to one at each lattice site, so that this system is always strongly correlated ( $U_{ff} \rightarrow \infty$ ). The hopping integral is scaled with the spatial dimension  $d$  so as to have a finite result in the limit [11]  $d \rightarrow \infty$ ; we measure all energies in units of  $t^* = 1$ . We work on a hyper cubic lattice where the noninteracting density of states is a Gaussian  $\rho(\varepsilon) = \exp(-\varepsilon^2)/\sqrt{\pi}$ . A chemical potential  $\mu$  is used to maintain the total electron filling  $n_{\text{tot}} = n_d + n_f$  at a constant value.

The solution of the Falicov–Kimball model has been described before in the literature [12–14] and will not be repeated here. Instead, we focus on the physical behavior of the exact solution. We present the results for the case where the total filling is  $n_{\text{tot}} = 1.5$  but the electrons can change from localized to itinerant (*i.e.*, we fix the total electron concentration not the individual electron concentrations). We choose values of the parameters [13, 14] where the system has a well defined crossover from a state at high temperature that has large  $f$ -occupancy ( $n_f \geq 0.36$  for  $T \geq 0.2$ ), to a state at low temperature with no  $f$ -electrons (for definition of the transition temperature  $T_V$ , see below). To open a gap in the DOS at high temperatures we need a large  $f$ – $f$  correlation and we choose  $U = 4$  (see below).

To model the low-temperature transition, we need to tune the renormalized  $f$ -electron level to lie just above the chemical potential as  $T \rightarrow 0$ , and to describe YbInCu<sub>4</sub>-like systems we choose several values of  $E_f$ . We find that the qualitative features of the results do not depend too strongly on the parameters in this regime (*i.e.*, if we choose another total electron filling  $1 \leq \rho_{\text{tot}} \leq 2$ , then we find similar results when we vary  $E_f$ ). As  $T$  increases, the large entropy of the local moments stabilizes the  $f$ -electron number and produces a large magnetic response of the system. We choose the Coulomb interaction of an  $f$ -electron with a conduction electron to be such that the density of states splits into two bands [13, 14]. The shape and the relative weight of the two bands depends on the band filling and temperature but the peak-to-peak distance between the lower and the upper band is always about  $U$ . The location of the  $f$ -level  $E_f$ , is the one parameter that we will adjust to control the high-temperature number of  $f$ -electrons (in the case of Eu) or  $f$ -holes (in the case of Yb). Note, the single-particle excitations are strongly renormalized by the Coulomb interaction, and the bare value of  $E_f$  has no physical meaning. Since the FK model neglects the hybridization, we use the variation of  $E_f$  to represent the change of the system due to the pressure or doping (chemical pressure). The gap in the density of states, which appears for  $U \geq 1.5$ , defines a characteristic energy scale  $T^*$ . The gap shrinks with the reduction of temperature but is fairly insensitive to the value of  $E_f$  which, on the other hand, has a drastic effect on  $T_V$ . For  $U = 4$  ( $U = 2$ ) we have  $T^* \simeq 2$  ( $T^* \simeq 0.4$ ) and  $T^* \simeq 1.6$  ( $T^* \simeq 0$ , a pseudo gap) at very high and low temperatures, respectively.

In this paper we consider the system with  $T^* \simeq 1.6$  ( $U = 4$ ) and discuss the temperature dependence of the spin susceptibility of  $f$ -electrons  $\chi(T)$ , the  $f$ -occupancy  $n_f(T)$ , the electrical resistance  $\rho_{\text{dc}}(T)$ , the thermoelectric power  $S(T)$ , and the thermal conductivity  $\kappa(T)$ , for five different values of  $E_f$ . We also discuss the frequency dependence of the optical conductivity  $\sigma(\omega)$ , the Raman response  $B_{1g}(\omega)$ , the magnetic field dependence of the  $f$ -electron magnetization  $m_f(h, T)$  and the electrical resistance  $R(h, T)$ , at several characteristic temperatures. The finite-frequency results are presented for  $E_f = -0.7$ , and the finite-field data for  $E_f = -0.6$ , which are fairly typical values.

## 2. Results and discussion

The first thing we show is a plot of  $\chi(T)$  and  $1/\chi(T)$ , which is a Curie-like law, but with a temperature-dependent concentration of spins  $\chi \propto n_f(T)/T$ . One can see from panel (a), in figure 1 that as  $E_f$  is made more negative, the peak in the susceptibility moves to lower  $T$  and the curves sharpen. We define the valence transition temperature  $T_V$  to be the temperature

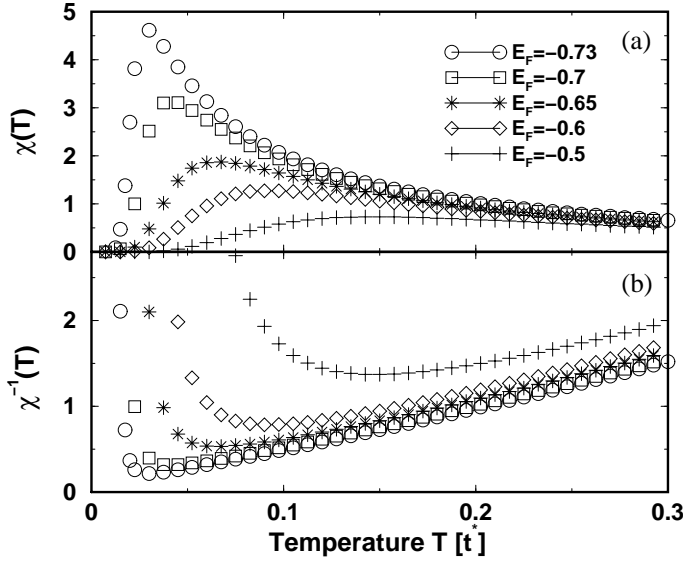


Fig. 1.  $f$ -electron magnetic susceptibility (a) and inverse susceptibility (b) for the Falicov–Kimball model with  $n_{\text{total}} = 1.5$  and  $U = 4$ . The symbols denote different values of  $E_f$ . These curves look remarkably like the experimental curves at high temperature (and through the transition).

below the peak in the susceptibility where  $\chi(T_V) = \chi(T_{\text{peak}})/2$ , *i.e.*, it is at the temperature corresponding to half the peak height of the susceptibility. This definition provides a well-defined benchmark for the value of  $T_V$  that is similar to choosing the inflection point of the susceptibility curves. All of the transitions we see here are actually smooth crossovers centered around  $T_V \ll T^*$ . We believe there is a region of parameters where the transition can be made discontinuous at low  $T$ , but the iterative algorithm normally used to solve this problem becomes unstable in the region close to such first-order transitions, and alternate methods need to be used to solve the problem. In panel (b) we plot the inverse susceptibility which shows the characteristic Curie or Curie–Weiss law at moderate temperatures (as  $E_f$  increases, the intercept of the Curie–Weiss law becomes more negative). Note that in our case there never is a low temperature turnover of the inverse susceptibility, since we plot only the  $f$ -electron susceptibility here, which vanishes as  $n_f \rightarrow 0$ . In  $\text{YbInCu}_4$  and  $\text{EuNi}_2(\text{Si}_{1-x}\text{Ge}_x)$ -like systems the ground state is a valence fluctuator with an enhanced Pauli susceptibility, such that the Curie plot shows a characteristic low- $T$  maximum.

In figure 2 we plot  $n_f(T)$ , which is relatively constant over a large temperature range and then suddenly drops toward zero at the transition. As  $E_f$  is made more negative, and the high-temperature  $f$ -filling is increased, the

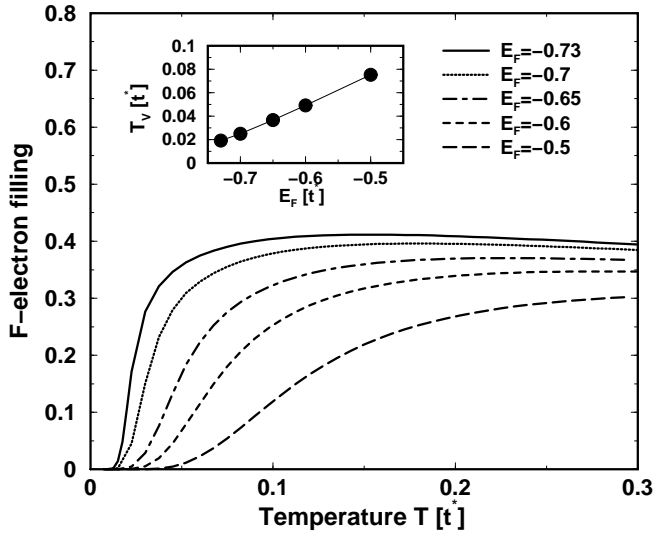


Fig. 2.  $f$ -electron filling versus temperature for the Falicov–Kimball model for the same parameters as in figure 2. The inset shows the valence transition temperature  $T_V$  versus the parameter  $E_f$ .

transition temperature  $T_V$  is reduced and the  $n_f(T)$ -curves sharpen. Note, the magnetic susceptibility, the particle number and the charge susceptibility, defined as  $\chi_c = \partial n_f / \partial \mu$ , reveal a characteristic scale  $T_V$  but do not provide any hint on the magnitude of  $T^*$ . The inset shows the correlation between  $T_V$  and  $E_f$ , which is our analog of experimental plots of  $T_V$  versus doping (for chemical pressure) or versus pressure. The behavior seen here, where applying pressure makes the  $E_f$  less negative and reduces the number of  $f$ -electrons, is similar to what would occur in experiment on Eu compounds;  $T_V$  increases along with a smoothing out of the susceptibility. In Yb-based systems, pressure has the opposite effect [2] on the properties of the system, since it increases the number of  $f$ -holes. As mentioned already, and discussed in detail in Refs. [13, 14], because of the FK interaction the temperature- or field-induced change in  $n_f$  leads to the MI transition in the conduction band, and is accompanied by substantial changes in the density of states. In the low-temperature phase, which is found for  $T < T_V$ , the weight of the upper conduction band is very small and the chemical potential is within the lower conduction band. In the high-temperature phase, which sets in for  $T > T_V$ , the spectral weight of the lower and upper band are about the same, and the chemical potential lies within the gap. Contrary to  $T_V$ , the characteristic temperature  $T^*$  is only weakly dependent on  $E_f$ .

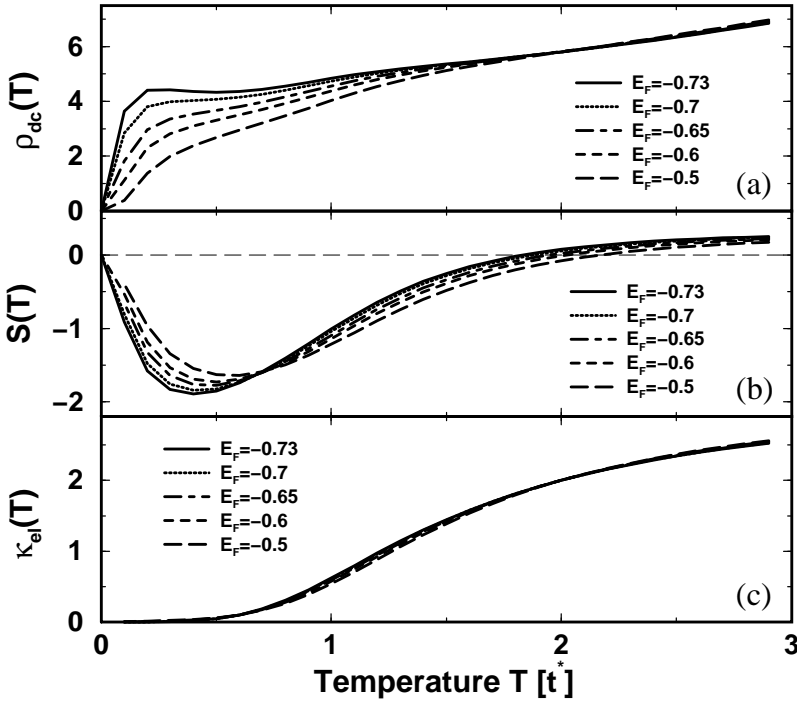


Fig. 3. DC conductivity (a), thermoelectric power (b), and thermal conductivity (c) for the spin-one-half Falicov–Kimball model as a function of temperature. The unrenormalized  $f$ -level is varied here to represent different doping or pressures. The high temperature phase is a poor metal with a moderate thermopower. At low temperatures, a normal metallic state develops. The thermal conductivity does not depend strongly on  $E_f$  in this parameter regime.

The DC transport properties in zero magnetic field, obtained by an exact evaluation of the current–current, current–heat current, and heat current–heat current correlation functions, are summarized in figure 3. We show  $\rho_{dc}(T)$ ,  $S(T)$ , and  $\kappa(T)$ , using the normalization that is usual for infinite dimensional lattices [15]. The thermopower is plotted for the hole-like Yb case; for the Eu compounds, the sign would have to be changed. The high temperature phase is a poor metal with a minimum in  $S(T)$  at about  $T^*/3$  and small hump in  $\rho_{dc}(T)$  at about  $T^*/2$  (do not confuse the hump at  $T \approx 1$  with the sharp low- $T$  decrease in  $\rho_{dc}$  that occurs near  $T_V$ ). Note, the thermopower does not exhibit any additional features around  $T_V$ . The minimum of  $S(T)$  decreases from  $T_{\min}=0.6$  to  $T_{\min}=0.4$ , as we change from  $E_f=-0.5$  ( $T_V=0.07$ ) to  $E_f=-0.73$  ( $T_V=0.03$ ), *i.e.* the relevant temperature scale for the thermoelectric power is set by  $T^*$  and not by  $T_V$ . In the  $U=2$  case,

which has the high-temperature gap  $T^* \simeq 0.4$ , the minimum of  $S(T)$  shifts from  $T_{\min} \simeq 0.4$  for  $E_f = -0.2$  ( $T_V = 0.25$ ) to  $T_{\min} \simeq 0.2$  for  $E_f = -0.6$  ( $T_V < 0.007$ ). The electronic part of the thermal conductivity shows a featureless decrease as temperature is reduced and no  $E_f$ -dependence. Thus, as long as  $T_V \leq T^*$ , the temperature scales revealed by the thermoelectric data and the thermodynamic data appear to be fundamentally different.

The temperature dependence of various correlation functions discussed above is remarkably similar to what one observes in  $\text{YbInCu}_4$  and  $\text{EuNi}_2(\text{Si}_{1-x}\text{Ge}_x)$ -like systems for  $T \geq T_V$ . The thermoelectric data obtained recently for  $\text{Yb}_{1-x}\text{Y}_x\text{InCu}_4$  and  $\text{YbAg}_x\text{In}_{1-x}\text{Cu}_4$  for various concentrations of Y and Ag dopants [3, 4] can be explained by the FK model, if we take the initial parameters for  $\text{YbInCu}_4$  such that  $T_V \simeq T^* \simeq T_{\min}$ , and assume that yttrium doping makes  $E_f$  more negative, while silver doping does the opposite. Note, the thermoelectric power of the low-temperature valence fluctuating phase is much larger than of the high-temperature semimetallic phase [3, 4], *i.e.* the heating of real systems across  $T_V$  always leads to a smaller  $S(T)$ .

The Y-doping pushes  $T_V$  (as defined by the susceptibility anomaly) to lower temperatures but does not change the position of the high-temperature minimum of  $S(T)$ , since  $T_{\min} \simeq T^* > T_V$ , and this does not depend on  $x$  or  $E_f$ . The thermoelectric power of  $\text{Yb}_{1-x}\text{Y}_x\text{InCu}_4$  exhibits two minima: a deep one at the temperature of the valence transition and shallow one at the temperature of the pseudo gap. The first one at  $T_V$  is doping-dependent, and the second one is doping-independent.

In  $\text{YbAg}_x\text{In}_{1-x}\text{Cu}_4$  one finds the valence transition for  $x \leq 0.3$ , and the silver doping enhances  $T_V$ , *i.e.*  $T_V(x) > T^*$ . The slope of  $S(T)$  in the valence-fluctuating phase is characterized by the Kondo scale  $T_K > T_V$ , and as the temperature increases up to  $T_V(x)$ , the thermo-power increases continuously up to large values. Above  $T_V$ ,  $S(T)$  drops to values typical of the high-temperature phase but since  $T > T_V > T^*$ , there is no high-temperature minimum of  $S(T)$ . Thus, as long as  $T_K > T_V > T^*$ , the thermopower has a single minimum at a temperature that coincides with the susceptibility maximum, and is strongly doping (or  $E_f$ ) dependent. However, Ag doping not only enhances  $T_V$  but also reduces  $T_K$ , and for  $x \geq 0.3$  the  $\text{YbAg}_x\text{In}_{1-x}\text{Cu}_4$  becomes a heavy fermion with  $T_K < T_V(x)$ . For  $T_K < T < T_V$ , the Kondo effect stabilizes the paramagnetic state before the valence transition takes place and the thermoelectric power exhibits the usual Kondo minimum at about  $T_K/2$ , that is not much changed by further doping. The effect of hydrostatic pressure on these compounds [2] follows from similar considerations, if we assume that pressure shifts  $E_f$  and reduces (increases) the average number of  $f$ -electrons ( $f$ -holes).



The transport properties of  $\text{EuNi}_2(\text{Si}_{1-x}\text{Ge}_x)_2$  compounds, which show [6, 7] (for  $0.7 \leq x \leq 0.8$ ) a valence transition at  $T_V(x) \geq 85$  K, can also be explained by the FK model, but with  $f$ -electrons rather than holes. The reduction of the Ge concentration shrinks the lattice, reduces the average value of  $f$ -electrons, increases  $T_V$ , and makes the susceptibility transition less sharp. In this electron-like system, the thermoelectric power is positive [6]. Since the maximum of  $S(T)$  is concentration dependent and  $T_{\text{max}} \simeq T_V$ , we would classify the high-temperature phase of  $\text{EuNi}_2(\text{Si}_{1-x}\text{Ge}_x)_2$  for  $0.7 \leq x \leq 0.8$ , as a small-gap FK state, with  $T^* \leq T_V$ .

In figure 4, we plot the optical conductivity [15]  $\sigma(\omega)$  and the  $B_{1g}(\omega)$  Raman response [16] for the case  $E_f = -0.7$  at a number of different temperatures. In the high temperature phase, the optical conductivity has the characteristic poor metal behavior, with a low-energy Drude-like feature

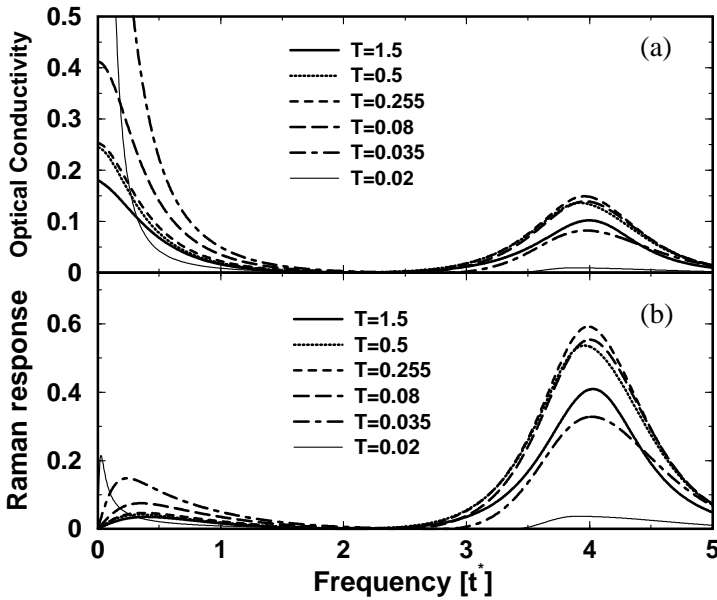


Fig. 4. Optical conductivity (a) and  $B_{1g}$  Raman response (b) of the spin-one-half Falicov-Kimball model with  $E_f = -0.7$  ( $T_V = 0.03$ ). Note how at high temperatures there is a separation of many-body excitations into a low-energy Drude-like peak and a higher-energy charge-transfer peak. As the temperature is lowered, spectral weight moves between these peaks, in an expected way for a sharpening of the “Fermi surface”, until one reaches  $T_V$  where the spectral weight changes dramatically, with the charge-transfer peak losing weight and the Drude peak being strongly enhanced. This last behavior is an artifact of not being able to describe the mixed-valence regime properly.

and a large weight charge-transfer peak around  $\omega \simeq U$ . As  $T$  is lowered, the scattering processes become sharpened, and both peaks grow in temperature. The charge-transfer peak is frozen in at around  $T = 0.5$ , but the Drude feature continues to increase. As  $T_V$  is approached, we see a transfer of weight from the charge-transfer peak to the Drude peak, which then becomes complete as  $T$  is lowered well below  $T_V$ . In this lowest temperature region, the results are not representative of real materials, as we expect there to still be a charge-transfer peak since the  $f$ -electrons have not gone into the conduction band, they have only hybridized with them. We also expect midinfrared excitations to appear, because the hybridization with the  $f$ -electrons will allow them to participate in the optical scattering, and the broadened  $f$ -spectral function should have weight in the midinfrared region. These latter features are seen in experiment on the Yb compounds. The Raman response behaves similarly, with a sharpening of the charge-transfer peak and the growth of a lower Fermi-liquid peak as  $T$  is lowered to  $T_V$ , where the spectral weight shifts become too large. Thus, the optical experiments can be used to estimate the value of  $U$ . We expect one would also see the turn on of the midinfrared response in the Raman scattering as  $T$  is lowered below  $T_V$  for the exact same reason it is seen in the optical conductivity.

If we estimate the  $f$ - $d$  correlation from the high-frequency peak in the optical conductivity and use the susceptibility results to define  $T_V$ , we obtain from figures 4 and 2 the ratio  $U/k_B T_V = 4/0.03 = 133$ . If we use model with  $U = 2$  and  $E_f = -0.6$ , the ratio is  $2/0.007 = 285$ . The optical data for YbInCu<sub>4</sub> crystals, with  $T_V \simeq 42$  K, exhibit the peak at  $12000 \text{ cm}^{-1}$  [9], which gives the experimental ratio  $U/T_V = 12000 \text{ cm}^{-1}/42 \text{ K} \simeq 375$ .

The field dependence of  $m_f(h, T)$  and  $R(h, T)$  is shown in figure 5 for  $U = 4$ ,  $E_f = -0.6$  ( $T_V \simeq 0.05$ ). Each curve corresponds to a different temperature, as indicated in the caption. For low temperatures and fields,  $m_f(h, T)$  and  $R(h, T)$  behave typically of a normal Fermi liquid. At high temperatures and high fields, however,  $m_f(h, T)$  behaves as expected of a non-interacting localized moment, while  $R(h, T)$  indicates a poor metal or a semiconductor. Figure 5 shows that the low-temperature metallic state is destroyed by large enough magnetic field. At a critical field  $H_c$  we find a metamagnetic transition in the  $f$ -subsystem and a metal-insulator transition in the conduction band. The  $H$ - $T$  phase boundary between the non-magnetic (metallic) phase and the paramagnetic (semimetallic) phase can be approximated by the expression  $H_c(T)/H_c^0 = \sqrt{1 - (2T/T_V)^2}$ , where the critical field  $H_c(T)$  is estimated from the midpoint of the magnetization curves shown in figure 5, and  $H_c^0$  is the critical field at  $T = 0$ . The ratio of the zero-temperature Zeeman energy at  $H_c^0$  and the zero-field thermal energy at  $T_V$  is  $\mu_B H_c^0/k_B T_V \simeq 2$ , where the gyromagnetic factor is  $g = 1$ , since

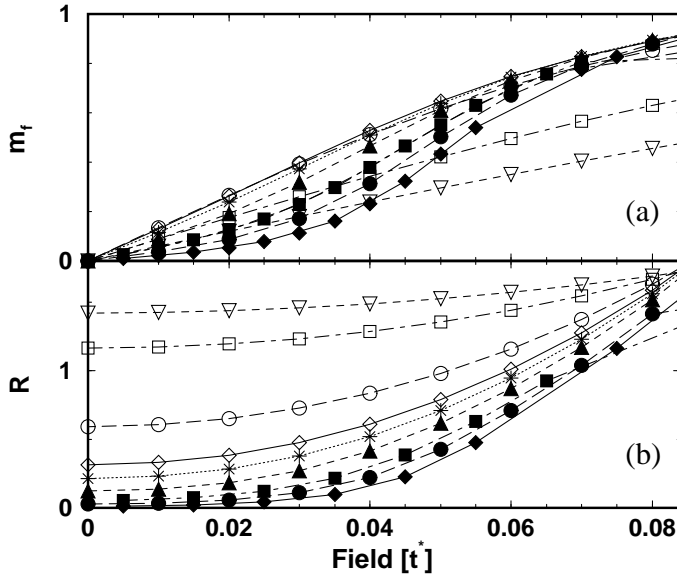


Fig. 5. Magnetic field dependence of the  $f$ -electron magnetization (a) and the electrical resistance (b) for the spin-one-half Falicov–Kimball model with  $n_{\text{total}} = 1.5$ ,  $U = 4$ ,  $E_f = -0.6$  ( $T_V = 0.05$ ). The filled symbols connected by the full, long-dashed, dashed-dotted, dashed and dotted line correspond to temperatures  $0.03t^*$ ,  $0.035t^*$ ,  $0.04t^*$ ,  $0.05t^*$ , and  $0.06t^*$ , respectively. The open symbols connected by the full, long-dashed, dashed-dotted, and dashed line correspond to temperatures  $0.07t^*$ ,  $0.1t^*$ ,  $0.2t^*$ , and  $0.3t^*$ , respectively.

we are interested in the Yb or Eu compounds which have the  $f$ -electrons in their lowest spin-orbit state. Thus, the high-field and the low-field data show the same characteristic energy scale.

### 3. Conclusions

We discuss the properties of  $\text{YbInCu}_4$  and  $\text{EuNi}_2(\text{Si}_{1-x}\text{Ge}_x)$ -like compounds using the exact solution the Falicov–Kimball model in infinite dimensions. In addition to the usual FK interaction, we include an infinitely large repulsion between  $f$ -particles of the opposite spin, which leads to  $n_f \leq 1$  ( $n_f$  describes electrons for Eu and holes for Yb). We consider the total filling  $n_{\text{tot}} = 1.5$ , and choose the parameters such that the ground state has a large  $d$ -electron spectral weight around the chemical potential  $\mu$  and a negligible  $f$ -occupancy. The mass of  $f$ -particles is assumed to be infinite but the  $f$ -level has a finite width because of the FK coupling to the density fluctuations in the conduction band. (Not surprising, this feature

is similar to what one finds in the X-ray edge problem, defined by a single impurity version of the FK Hamiltonian.) The spectral functions of the  $f$ - and  $d$ -states are gapped and the spectral weight is strongly temperature- and field-dependent. At low temperatures, there are many more conduction states below than above the gap, while for the  $f$ -states just the opposite is true. At high temperatures, the chemical potential is in the gap, and the weight of the occupied and unoccupied the  $d$ - and  $f$ -states are about the same.

The FK model predicts a valence transition at  $T_V$ , a metamagnetic transition for the  $f$ -electron magnetization at  $H_C$ , and a metal-insulator transition in the conduction band, such that the high-temperature, high-field transport is dominated by a pseudo gap or a gap  $\sim T^*$ . The paramagnetic, semimetallic phase sets in because of thermal population of highly-degenerate  $f$ -states, which can be understood as an entropy driven transition. The proximity of the renormalized  $f$ -state to the chemical potential explains the sensitivity of the transition to an external field, doping or pressure. By tuning the position of the  $f$ -level, the transition can be pushed to low temperatures, where it becomes very sharp.

For  $T > T_V$ , the number of  $f$ -particles is large and only weakly temperature dependent. The zero-field susceptibility is given by the Curie law,  $\chi(T) \simeq n_f(T)/T$ , rather than the Curie-Weiss law, *i.e.* the Curie plot gives only a small Curie-Weiss temperature and a “Curie constant” that depends on the thermal occupation of the excited  $f$ -states. Note, the presence of the local moment in the high-temperature phase is not accompanied by the usual Kondo anomalies in the electronic transport, since the model has no  $f$ - $d$  mixing. The calculated electrical resistance is large with a positive (temperature) slope, the magnetoresistance is positive, and the thermoelectric power is small with a peak at about  $T \simeq T^*$ . The optical conductivity has a pronounced peak at  $\omega \simeq U$  and a suppressed Drude peak, as expected of a strongly correlated semimetal. Most of these features are observed in the high-temperature, high-field phase of  $\text{YbInCu}_4$  and  $\text{EuNi}_2(\text{Si}_{1-x}\text{Ge}_x)$ -like compounds and they seem to characterize a new fixed point of strongly correlated electrons.

The low-temperature, low-field properties of the FK model correspond to a metal with a Pauli susceptibility, usual DC transport with a small thermoelectric power, and a large Drude peak in the optical conductivity. However, the model neglects the  $d$ - $f$  hybridization and its low-temperature metallic phase without the  $f$ -particles, cannot describe the low-temperature state of intermetallic compounds with Eu and Yb ions. The physical ground state is a valence fluctuator with a large average  $f$ -occupancy, an enhanced Pauli susceptibility, huge thermoelectric power, and an additional midinfrared peak in the optical conductivity. All these features follow from the

periodic Anderson model with an infinite  $f$ - $f$  correlation and a  $d$ - $f$  hybridization. In that model, the proximity of the  $d$  and  $f$  spectral weight to the chemical potential leads to  $d$ - $f$  inter-band transitions and a mid-infrared peak in  $\sigma(\omega)$ . It appears that the low-temperature phase of the above mentioned compounds can be explained by the PAM, and the  $f$ - $d$  correlation can be neglected.

On the other hand, the semimetallic high-temperature phase of  $\text{YbInCu}_4$  and  $\text{EuNi}_2(\text{Si}_{1-x}\text{Ge}_x)$  is difficult to describe in terms of the usual solutions of the PAM, which can lead to a fluctuating local  $f$ -moment but always keeps the  $d$ -electrons metallic. The absence of the Kondo effect in the electrical resistance, the magnetoresistance and the thermoelectric power data is difficult to reconcile with the susceptibility data which is typical of local moments with a small Curie-Weiss temperature. Such a behavior is not easy to explain in terms of conduction electrons that exchange scatter on the localized  $f$ -moments. As long as the  $f$ -state overlaps the continuum of metallic states, the quantum mixing leads to the Kondo effect, and that is not seen in the high-temperature phase of  $\text{YbInCu}_4$  and  $\text{EuNi}_2(\text{Si}_{1-x}\text{Ge}_x)$ -like compounds. Also, it is not clear that the PAM could provide a sharp transition from a metallic (mixed valence, non-magnetic) state to a semimetallic (integral valence, paramagnetic) state, as observed experimentally. In our approach, we argue that the high-temperature width and the weight of the  $f$ -spectral function below the gap is very large, such that the additional broadening due to the  $f$ - $d$  mixing can be neglected. In that sense, the FK model can be considered as an effective model for the high-temperature phase of a generalized periodic Anderson model which, in addition to the usual  $f$ - $f$  correlations and  $f$ - $d$  hybridization, also has the  $f$ - $d$  correlation. It would be interesting to study the low temperature fixed point of such a generalized periodic Anderson model with the Falicov-Kimball term, to see if it reduces to the usual valence fluctuating fixed point of the periodic Anderson model.

We acknowledge support of the National Science Foundation under grant no. DMR-9973225. We also acknowledge useful discussions with S.L. Cooper, G. Czycholl, C. Geibel, M. Očko and J. Sarrao.

## REFERENCES

- [1] I. Felner, I. Novik., *Phys. Rev.* **B33**, 617 (1986).
- [2] J.L. Sarrao, *Physica*, **B259&261**, 129 (1999).
- [3] M. Očko, D. Drobac, J.L. Sarrao, *Phys. Rev.* **B64**, 085103 (2001).
- [4] M. Očko, J.L. Sarrao, *Physica B*, in press (2001).
- [5] E. Figueroa *et al.*, *Solid State Commun.* **106**, 347 (1998).
- [6] E.M. Levin, B.S. Kuzhel, O.I. Bodak, B.D. Belan, I.N. Stets, *Phys. Status Solidi* **B161**, 783 (1990).
- [7] H. Wada, A. Nakamura, A. Mitsuda, M. Shiga, T. Tanaka, H. Mitamura, T. Goto, *J. Phys. Condens. Matter* **9**, 7913 (1997).
- [8] A. Severing, E. Gratz, B.D. Rainford, K. Yoshimura, *Physica* **B163**, 409 (1990).
- [9] S.R. Garner, J.N. Hancock, Y.W. Rodriguez, Z. Schlesinger, B. Bucher, Z. Fisk, J.L. Sarrao, *Phys. Rev.* **B62**, R4778 (2000).
- [10] L. M. Falicov, J. C. Kimball, *Phys. Rev. Lett.* **22**, 997 (1969).
- [11] W. Metzner, D. Vollhardt, *Phys. Rev. Lett.* **62**, 324 (1989).
- [12] U. Brandt, C. Mielsch, *Z. Phys.* **B75**, 365 (1989); U. Brandt, M.P. Urbanek, *Z. Phys.* **B89**, 297 (1992).
- [13] J. Freericks, V. Zlatić, *Phys. Rev.* **B58**, 322 (1998); V. Zlatić, J.K. Freericks, *Open Problems in Strongly Correlated Electrons*, Eds. J. Bonča, A. Ramšak, P. Prelovšek and S. Sarkar, NATO Science Series II: Mathematics, Physics and Chemistry, Vol. 15, Kluwer Academic Publishers, Dordrecht 2001.
- [14] V. Zlatić, J.K. Freericks, R. Lemański, G. Czycholl, *Philos. Mag.* **B81**, 1443 (2001).
- [15] Th. Pruschke, M. Jarrell, J.K. Freericks, *Adv. Phys.* **44** 187 (1995).
- [16] J.K. Freericks, T.P. Devereaux, *J. Condens. Phys.* **4**, 149 (2001); submitted to *Europhys. Lett.* (cond-mat/0011013); to appear in *Phys. Rev. B*; (cond-mat/0104047).